

Study of nuclear modification factors of (anti)hadrons and light (anti)nuclei in Pb-Pb collisions at $\sqrt{s_{NN}} = 2.76$ TeV

Zhi-Lei She^{1,2}, Gang Chen^{2*}, Feng-Xian Liu^{1,2}, Liang Zheng² and Yi-Long Xie²

¹*Institute of Geophysics and Geomatics, China University of Geosciences, Wuhan 430074, China*

²*School of Mathematics and Physics, China University of Geosciences, Wuhan 430074, China*

(Dated: Received: date / Accepted: date)

The nuclear modification factors (R_{AA}) of $\pi^\pm, p(\bar{p})$, and $d(\bar{d})$ with $|y| < 0.5, p_T < 20.0$ GeV/c in peripheral (40-60%) and central (0-5%) Pb-Pb collisions at $\sqrt{s_{NN}} = 2.76$ TeV have been studied using the parton and hadron cascade (PACIAE) model plus the dynamically constrained phase space coalescence (DCPC) model. It is found that the R_{AA} of light (anti)nuclei (d, \bar{d}) is similar to that of hadrons (π^\pm, p, \bar{p}), and the R_{AA} of antiparticles is the same as that of particles. The suppression of R_{AA} at high- p_T strongly depends on event centrality and mass of the particles, i.e., the central collision is more suppressed than the peripheral collision. Besides, the yield ratios and double ratios for different particle species in pp and Pb-Pb collisions are discussed, respectively. It is observed that the yield ratios and double ratios of d to p and p to π are similar to those of their anti-particles in three different collision systems, suggesting that the suppressions of matter (π^+, p, d) and the corresponding antimatter (π^-, \bar{p}, \bar{d}) are around the same level.

PACS numbers: 25.75.-q, 24.85.+p, 24.10.Lx

I. INTRODUCTION

It is known that quark-gluon plasma (QGP), a new form of nuclear matter characterized by the deconfined state of quarks and gluons, can be produced in heavy-ion collisions at ultra-relativistic energies, such as at the Relativistic Heavy-Ion Collider (RHIC) at BNL and Large Hadron Collider (LHC) at CERN. Since a large amount of energy is deposited in the extended QGP matter, it is allowed to create abundant anti-matter ranging from hadrons to light nuclei. Quantitative studies on the production of anti-matter in high energy heavy ion collisions will shed light on the understanding to the anti-matter to matter asymmetry in our universe. Up to now, numerous experimental results of (anti)hadrons ($\pi^-, \bar{p}, \bar{\Lambda}$, etc.) and (anti)nuclei ($\bar{d}, {}^3\bar{H}e$, and $\frac{3}{\Lambda}\bar{H}$, etc.) in pp [1–3] and Pb-Pb [1, 2, 4–8] collisions at $\sqrt{s_{NN}} = 2.76$ TeV have been reported.

Transverse momentum spectra of various particle species in nucleus-nucleus (A-A) collisions can be applied to study many important properties of the QGP matter. The microscopic process at low p_T is dominant by the bulk production. In the intermediate p_T region, the baryon-to-meson ratio shows an enhancement [9–11], which is the so called "baryon anomaly" not fully understood so far. For the inclusive particle spectra at high p_T , transport properties of the QGP matter can be obtained through jet quenching [12–14]. Experimentally, the nuclear modification factor R_{AA} is usually performed to study the jet quenching effect [1, 15–19].

The R_{AA} , which compares the p_T distributions of the charged particles in nucleus-nucleus (A-A) collisions to

pp collisions, is typically expressed as [2]:

$$R_{AA}(p_T) = \frac{d^2 N_{id}^{AA} / d\eta dp_T}{\langle T_{AA} \rangle d^2 \sigma_{id}^{pp} / d\eta dp_T}. \quad (1)$$

where N_{id}^{AA} and σ_{id}^{pp} denote the charged particles yield per event in A-A collision and the cross section in pp collision, respectively. The nuclear overlap function T_{AA} is computed based on the Glauber model [20].

The study of the R_{AA} plays an important role in understanding the detailed mechanism by which hard partons lose energy traversing the medium [21]. Recent experimental data of R_{AA} in Pb-Pb collision from ALICE [1, 2, 17, 18, 22] and CMS [19] experiments have been published for a range of charged hadrons. Compared with R_{AA} of hadrons (charged particles, π, k, p , etc.), R_{AA} of light (anti)nuclei is not well explained in high energy A-A collision experiments. Therefore we think the properties of R_{AA} of (anti)hadrons and (anti)nuclei in Pb-Pb collisions deserve to be further discussed in models.

Presently, there are many successful phenomenological models widely used to describe the production of hadrons and light nuclei in relativistic heavy-ion collisions [23, 24], such as the Ultra-relativistic Quantum Molecular Dynamics (UrQMD) approach [25], a Multiphase Transport (AMPT) model [26], and the Simulating Many Accelerated Strongly interacting Hadrons (SMASH) approach [27]. For the light (anti)nuclei production in terms of their yields, yield ratios, spectra, flow, etc, coalescence models and statistical thermal method are usually employed, as has been done in the frameworks of either the coalescence approach [28–35] or the statistical model approach [36–39].

In this paper, the production and transverse momentum (p_T) of final state (anti)hadrons (π^+, π^-, p, \bar{p}) are simulated by the PACIAE model [40] in pp and Pb-Pb collisions at $\sqrt{s_{NN}} = 2.76$ TeV. And then the dy-

*Corresponding Author: chengang1@cug.edu.cn

namically constrained phase-space coalescence (DCPC) model [41] is applied to deal with the production and properties of light (anti)nuclei (d, \bar{d}). Previous results of light (anti)nuclei production for both pp [41, 42] and A-A [43–49] collisions in relativistic energy region, including transverse momentum distribution, energy dependence, scaling property, centrality dependence have been obtained using this framework. In the rest of this paper, we will investigate the properties of nuclear modification factors (R_{AA}) of (anti)hadrons and (anti)deuteron in Pb-Pb collisions at $\sqrt{s_{NN}} = 2.76$ TeV with the same approach.

The paper is organized as follows: In sect. II, we concisely introduce the PACIAE and DCPC model. In sect. III, our numerical calculation results of the R_{AA} for (anti)hadrons and (anti) deuteron are presented and compared with the available experimental data at LHC. In sect. IV, a brief summary is provided.

II. MODELS

The PACIAE model [40] based on PYTHIA 6.4 [50], is designed and expanded to be feasible for p-p, p-A and A-A collisions. In this model, the entire collision process can be mainly decomposed into four stages as follows:

Firstly, the partonic initial states are created. The nucleus-nucleus collision can be simplified into numerous nucleon-nucleon (NN) collisions according to the collision geometry and NN total cross section. Each NN collision is described by the PYTHIA model generating quarks and gluons for further evolution. A partonic initial state of a nucleus-nucleus collision can be created when all NN collisions are exhausted. This state is also considered as the quark-gluon matter (QGM) generated in high energy nucleus-nucleus collisions. Secondly, the parton rescattering proceeds via the $2 \rightarrow 2$ parton-parton scattering described by the LO-pQCD cross sections [51]. Here, a K factor is added to include non-perturbative QCD and higher-order corrections. Thirdly, the hadronization process is treated through the Lund string fragmentation approach [50] or the phenomenological coalescence method [40]. Finally, the hadron rescattering is carried out till the exhaustion of hadron-hadron collision pairs or the hadronic freeze-out. One refers to [40] for the detail.

Then the production of light (anti)nuclei can be calculated with the DCPC model [41] when the final state hadrons have already been provided by PACIAE. Due to the uncertainty principle ($\Delta\vec{q}\Delta\vec{p} \geq h^3$), one cannot simultaneously obtain the precise information of both position $q \equiv (x, y, z)$ and momentum $p \equiv (p_x, p_y, p_z)$ for a particle in the six-dimension phase space. Thus one can only deduce that this particle lies in a quantum "box" with a phase-space volume of $\Delta\vec{q}\Delta\vec{p}$. Hence we can simulate the yield of a single particle using an integral:

$$Y_1 = \int_{H \leq E} \frac{d\vec{q}d\vec{p}}{h^3}, \quad (2)$$

where H and E denote the Hamiltonian and energy of the particle, respectively. Analogously, one can compute the yield of the synthetic (anti)nuclei containing N particles with the following integral:

$$Y_N = \int \dots \int_{H \leq E} \frac{d\vec{q}_1 d\vec{p}_1 \dots d\vec{q}_N d\vec{p}_N}{h^{3N}}. \quad (3)$$

Note that, two constraint conditions have to be satisfied in this equation:

$$m_0 \leq m_{inv} \leq m_0 + \Delta m, \quad (4)$$

$$|q_{ij}| \leq D_0, (i \neq j; i, j = 1, 2, \dots, N) \quad (5)$$

where

$$m_{inv} = \left[\left(\sum_{i=1}^N E_i \right)^2 - \left(\sum_{i=1}^N \vec{p}_i \right)^2 \right]^{1/2}, \quad (6)$$

and $E_i, \vec{p}_i (i = 1, 2, \dots, N)$ represent the energy and momentum of one particle, respectively. m_0 and Δm denote the rest mass of synthetic (anti)nuclei and the allowed mass uncertainty. D_0 refers to diameter of (anti)nuclei, and $|q_{ij}|$ stands for the vector distance from i -th and j -th particles. The integration in Eq. (3) should be replaced by the summation over discrete distributions, as a coarse graining process in the transport model.

III. RESULTS AND DISCUSSIONS

At first, we can obtain the final-state particles in pp and Pb-Pb collisions using the PACIAE model [40]. In this simulation, the hadrons are created on the assumption that hyperons heavier than Λ are already decayed, and most of model parameters are fixed on the default values given in PYTHIA6.4 [50]. We determine the K factor, $\text{parj}(1,2,3)$ for primary hadrons in PACIAE model by fitting to the ALICE pions and protons p_T spectra data [2]. The fitted values of $K = 2$, $\text{parj}(1) = 0.15$, $\text{parj}(2) = 0.50$, and $\text{parj}(3) = 0.60$ for pp collisions as well as $K = 2$, $\text{parj}(1) = 0.15$, $\text{parj}(2) = 0.38$, and $\text{parj}(3) = 0.65$ for Pb-Pb collisions are used in later calculations. Here, $\text{parj}(1)$ is the suppression of diquark-antidiquark pair production compared with the quark-antiquark pair production, $\text{parj}(2)$ is the suppression of strange quark pair production compared with u (d) quark pair production, and $\text{parj}(3)$ is the extra suppression of strange diquark production compared with the normal suppression of a strange quark. Then we generate charged pions and (anti)protons transverse momentum spectra by PACIAE model with $|y| < 0.5$ and $0 < p_T < 20$ GeV/c at $\sqrt{s_{NN}} = 2.76$ TeV, in pp collisions as shown in Fig. 1 and Pb-Pb collisions for centrality bin of 0-5% and 40-60% as shown in Fig. 2, respectively.

Then the yields and transverse momentum spectra of (anti)deuteron were calculated by the dynamically constrained phase-space coalescence model (DCPC) in pp

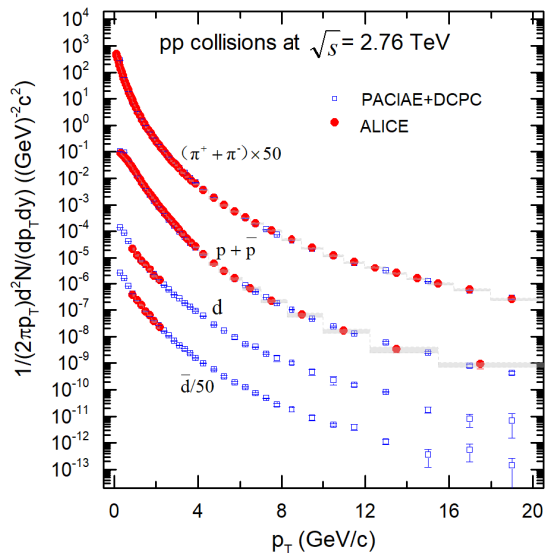


FIG. 1: (Color online) The transverse momentum spectra of charged pions, (anti)protons, and (anti)deuteron computed by PACIAE+DCPC model (the open symbols) in pp collisions at $\sqrt{s} = 2.76$ TeV, compared with ALICE results [2, 3] (the solid symbols). The vertical lines (error bars) show the statistical uncertainty and the shaded areas represent the systematic uncertainty of the ALICE results. The spectra have been scaled by the factors listed in the legend for clarity.

and Pb-Pb collisions at $\sqrt{s_{NN}} = 2.76$ TeV according to the final hadronic states from the PACIAE model. Here, we choose the model parameter $D_0 = 3$ fm and $\Delta m = 0.42$ MeV/c in pp and Pb-Pb collisions [46]. In the end, we can compare the model calculations of the nuclear modification factors for (anti)hadrons and light (anti)nuclei in Pb-Pb collisions at $\sqrt{s_{NN}} = 2.76$ TeV to experimental data and study the quenching effect in relativistic heavy ion collisions.

In Fig. 1, the transverse momentum spectra of charged pions, and (anti)protons computed by PACIAE model (the open symbols) in pp collisions at $\sqrt{s} = 2.76$ TeV within rapidity $|y| < 0.5$ were used to fit model parameters with ALICE results [2] (the solid symbols). In addition, the transverse momentum spectra of (anti)deuteron calculated by the PACIAE+DCPC model simulation (the open symbols) in pp collisions at $\sqrt{s} = 2.76$ TeV within rapidity $|y| < 0.5$ are also shown in the Fig. 1, which is in good agreement with the known ALICE results [3].

Similarly, Fig. 2 shows the transverse momentum spectra of charged pions, and (anti)protons calculated by PACIAE+DCPC model (open symbols) in Pb-Pb collisions at $\sqrt{s_{NN}} = 2.76$ TeV for different centrality bins of 0-5% and 40-60% within rapidity $|y| < 0.5$ confronted with ALICE results [2] (the solid symbols). One can see from Fig. 2 that for $p_T < 3.0$ GeV/c, the spectra in central collisions becomes harder and there is a mass dependent effect. Both protons and pions p_T spectra are well described by our model in different centrality bins. Then

the transverse momentum spectra of deuteron computed by the PACIAE+DCPC model simulation (the open symbols) in Pb-Pb collisions at $\sqrt{s_{NN}} = 2.76$ TeV in both central and peripheral collisions are in good agreement with the ALICE data [6, 7] as shown in Fig. 2.

The nuclear modification factor R_{AA} for pion, proton and deuteron is shown in Fig. 3 (the open symbols). Figure 3 (a) to (c) show the distribution of the nuclear modification factor R_{AA} for the π^+ , p , and d compared to their antiparticles π^- , \bar{p} , and \bar{d} , in two different centrality bins. Figure 3 (d) to (f) show the distribution of R_{AA} versus p_T for combined $\pi^+ + \pi^-$, $p + \bar{p}$, and $d + \bar{d}$.

From Fig. 3, one can see that the distribution of the nuclear modification factor R_{AA} for different particle species and different centrality increases with p_T value, reaches a peak, and then decreases with transverse momentum p_T , indicating a unified energy loss mechanism is acting on all the different particle species including nuclei at high transverse momentum. And the depression effect of central collision event are more significant than that of peripheral collision, due to a stronger medium modification effect in central collisions. Next, we can see from Fig. 3 (a) to (c) that the R_{AA} distribution of antihadrons and antinuclei are the same with that of corresponding hadrons and nuclei, showing that the R_{AA} suppression or quenching effect on matter and antimatter is the same in high energy Pb-Pb collisions. It is worth noting, as shown in Fig. 3 (c) and (f), that the suppression or quenching effect in the high transverse momentum region is more significant for nuclei than in meson and baryons.

The solid markers in Fig. 3 (c), (d), and (e) represent the experimental data [2, 3, 6] compared with our simulation results. It is observed that the R_{AA} results of the $\pi^+ + \pi^-$, $p + \bar{p}$ and d from our simulation are comparable to those of the ALICE data at $p_T < 10.0$ GeV/c within the current errors in Fig. 3 (c), (d), (e); while as $p_T > 10.0$ GeV/c, our simulation is off the data by a small factor. It should be mentioned that the ALICE data $R_{AA}(d)$ used for comparison in Fig. 3 (c) were calculated according to Eq. (1) based on the experimental data taken from Ref. [3] for pp collisions and Ref. [6] for Pb-Pb collisions.

We also perform a particle ratio study versus p_T for (anti)proton to charged pion and (anti)deuteron to (anti)proton in this model. Figure 4 (a) and (b), display the ratio distributions of p/π^+ , \bar{p}/π^- , d/p , and \bar{d}/\bar{p} , respectively. It's easy to see that the distributions of the ratio for p/π^+ , d/p are similar to \bar{d}/\bar{p} , \bar{p}/π^- in pp collisions, central and peripheral Pb-Pb collisions, suggesting a common suppression behavior for the matter and antimatter.

The ratio distributions of $p + \bar{p}/\pi^+ + \pi^-$ and $d + \bar{d}/p + \bar{p}$ are shown in Fig. 4 (c) and (d). It can be seen that for the central and peripheral Pb-Pb collisions, the ratio grows to a maximum value at $p_T \sim 3.0$ GeV/c for $(p + \bar{p})/(\pi^+ + \pi^-)$ and $p_T \sim 5.0$ GeV/c for $(d + \bar{d})/(p + \bar{p})$, then decreases as p_T increases. In Fig. 4 (c) and (d), the

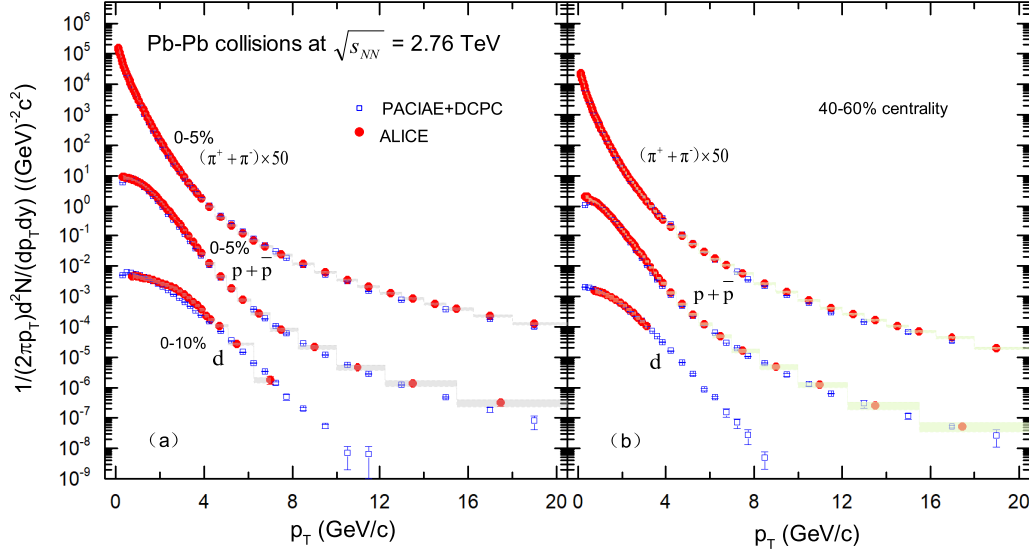


FIG. 2: The transverse momentum spectra of charged pions, (anti)protons, and deuterons are presented by PACIAE+DCPC model (the open symbols) in Pb-Pb collisions at $\sqrt{s_{NN}} = 2.76$ TeV, compared with ALICE results [2, 6, 7] (the solid symbols), (a) in centrality bin of 0-5% for $\pi^+ + \pi^-$, $p + \bar{p}$ and 0-10% for d , (b) in centrality bin of 40-60%, respectively. The vertical lines (error bars) show the statistical uncertainty and the shaded areas represent the systematic uncertainty of the experimental results. The spectra of charged pions have been scaled by the factors 50 for clarity.

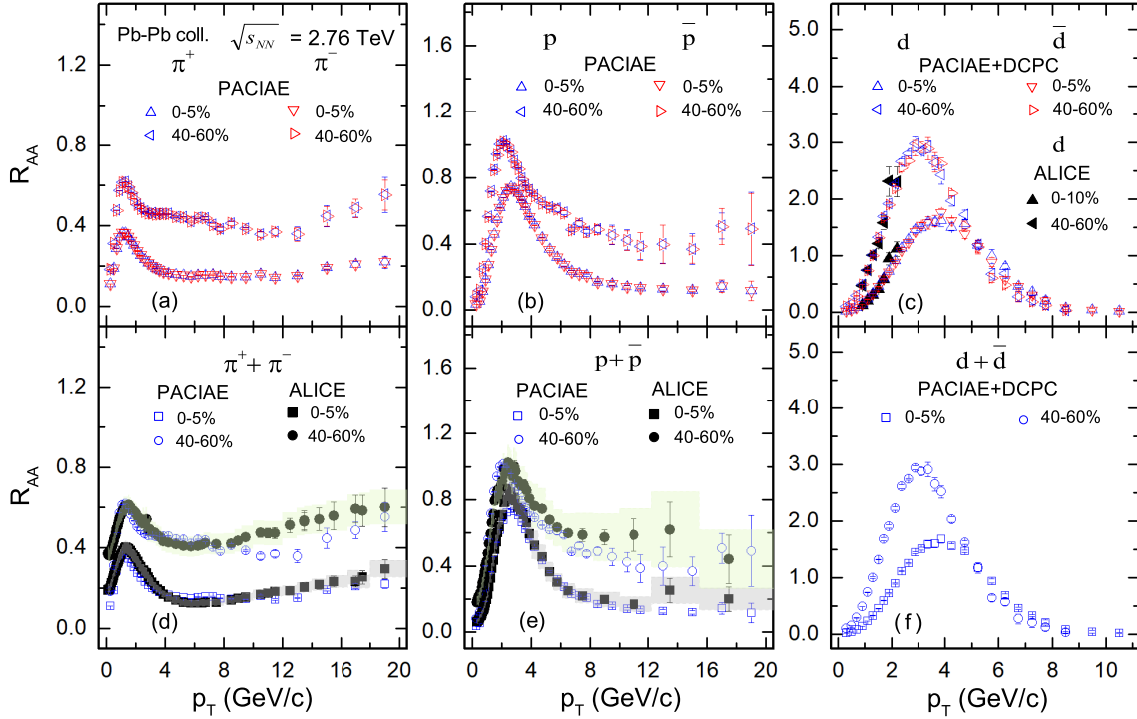


FIG. 3: (Color online) The nuclear modification factor R_{AA} are calculated by PACIAE+DCPC model (the open symbols) for different particle species in 0-5% most central and 40-60% peripheral Pb-Pb collision events at $\sqrt{s_{NN}} = 2.76$ TeV, as a function of p_T . The ALICE results (the solid markers) for comparison were taken from Ref. [2] for panel (d) and (e), and were computed using the data from Ref. [3, 6] for panel (c). The vertical lines (error bars) show the statistical uncertainty and the shaded areas represent the systematic uncertainty of the experimental results.

solid markers show the ALICE results [2] for comparison. Obviously, the $p + \bar{p}/\pi^+ + \pi^-$ ratio in our simulation

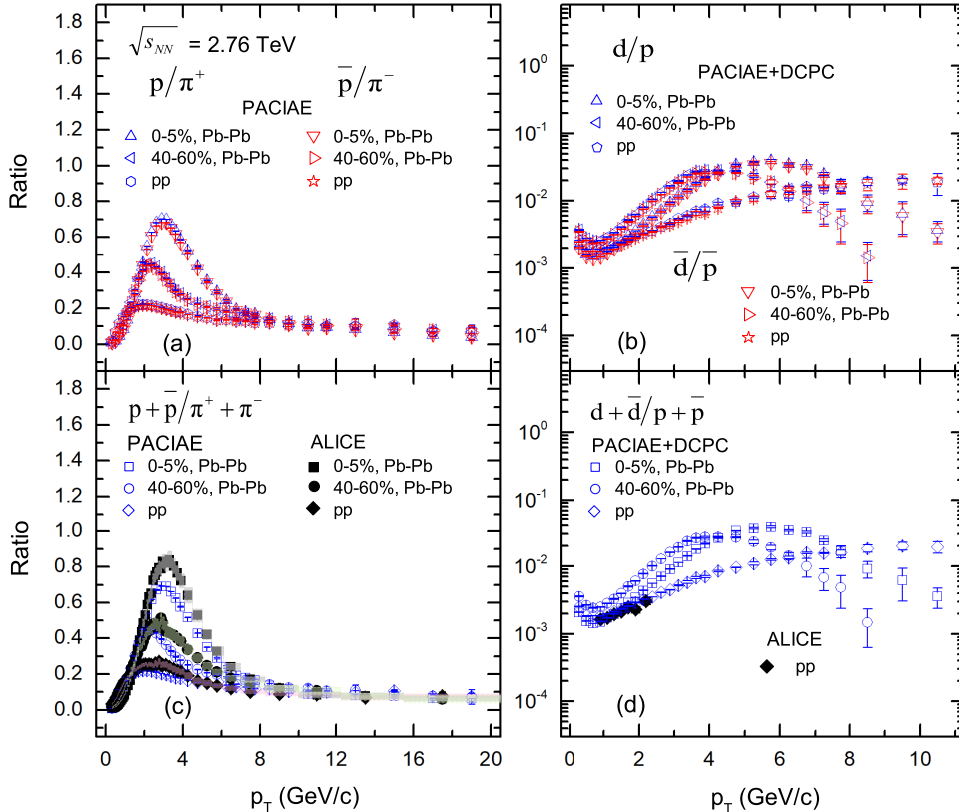


FIG. 4: The ratios of (anti)proton to charged-pion and (anti)deuteron to (anti)proton computed by PACIAE+DCPC model (the open symbols) as a function of p_T in pp collisions, as well as the most central (0-5%) and peripheral (40-60%) Pb-Pb collisions at $\sqrt{s_{NN}} = 2.76$ TeV, respectively. Here, ALICE results (the solid markers) for comparison were taken from Ref. [2] in panel (c), and were computed with the data from Ref. [2, 3] in panel (d). The vertical lines (error bars) show the statistical uncertainty and the shaded areas represent the systematic uncertainty of the experimental results.

shows a similar structure to that in data. The ALICE data ($d + \bar{d}/p + \bar{p}$) used for comparison in Fig. 4 (d) were computed using data ($p + \bar{p}$) taken from Ref. [2] and data ($d + \bar{d}$) from Ref. [3].

To quantify the similarity of the suppression, the double R_{AA}^D ratio were defined, such as the double ratio R_{AA}^D of protons to pions is defined as follows [1]:

$$R_{AA}^D = \frac{R_{AA}^{p+\bar{p}}}{R_{AA}^{\pi^++\pi^-}}, \quad (7)$$

where $R_{AA}^{\pi^++\pi^-}$ and $R_{AA}^{p+\bar{p}}$ denote the R_{AA} for the charged pion and proton, respectively. This double ratios constructed using the particle ratios may be properly handled that the dominant correlated systematic uncertainties are between particle species and not between different collision systems.

Fig. 5 shows the double R_{AA}^D ratios of protons ($p, \bar{p}, p + \bar{p}$) to pions ($\pi^+, \pi^-, \pi^+ + \pi^-$) and deuterons ($d, \bar{d}, d + \bar{d}$) to protons ($p, \bar{p}, p + \bar{p}$), as a function of p_T , calculated by PACIAE+DCPC in the most central (0-5%) and peripheral (40-60%) Pb-Pb collisions at $\sqrt{s_{NN}} = 2.76$ TeV, respec-

tively. We can see from Fig. 5, that the R_{AA}^D for all particle combinations are generally increasing at low p_T and decreasing at high p_T . And comparing Fig. 5 (a),(c) with Fig. 5 (b),(d), we can also conclude that the suppression effect of the double R_{AA}^D ratio of deuteron to proton is more significant than that of proton to pion, as $p_T > 8$ GeV/c. Besides, it is clear that, as shown in Fig. 5 (a) and (b), the distribution of the double R_{AA}^D ratios for p to π^+ and d to p are the same as that of corresponding antimatter \bar{p} to π^- and \bar{d} to \bar{p} , which indicates that matter and corresponding antimatter have the same suppression characteristics. Meanwhile, from Fig. 5 (c) it can be seen that the distribution of the results R_{AA}^D from computed by model simulation are consistent with the ALICE data [1, 2]. It should be noted that the experimental values of double ratios $R_{AA}^{p+\bar{p}}/R_{AA}^{\pi^++\pi^-}$ used for comparison in Fig. 5 (c), when $p_T < 4.0$ GeV/c, were calculated using data $R_{AA}^{p+\bar{p}}$ and $R_{AA}^{\pi^++\pi^-}$ taken from Ref. [2], and when $p_T > 4.0$ GeV/c, were taken directly from Ref. [1].

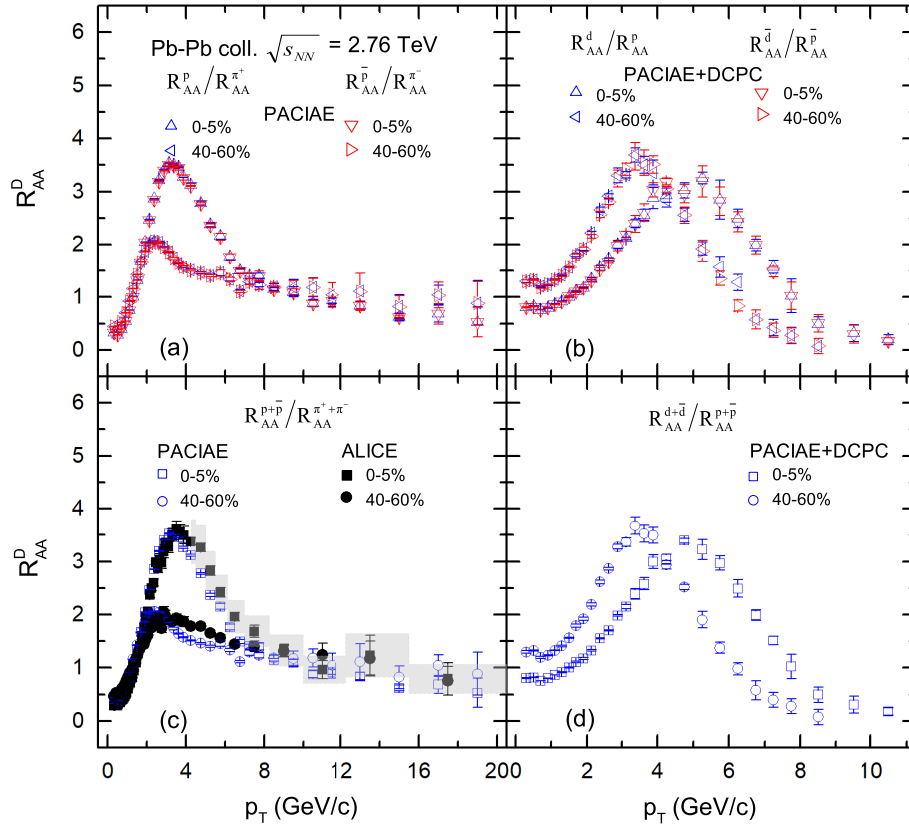


FIG. 5: The double ratios R_{AA}^D of (anti)proton to charged-pion and (anti)deuteron to (anti)proton computed by PACIAE+DCPC model (the open symbols) as a function of p_T in pp collisions, as well as in Pb-Pb collisions of the centrality bins of 0-5% and 40-60% at $\sqrt{s_{NN}} = 2.76$ TeV, respectively. Here, ALICE data (the solid markers) for comparison in panel (c), at $p_T > 4.0$ GeV/c, were taken directly from Ref. [1]; at $p_T < 4.0$ GeV/c, were calculated using the data from Ref [2]. The vertical lines (error bars) show the statistical uncertainty and the shaded areas represent the systematic uncertainty of the experimental results.

IV. CONCLUSIONS

In the paper, we have studied the transverse momentum (p_T) spectra of charged particles $\pi^+ + \pi^-$ and $p + \bar{p}$ at scaled midrapidity $|y| < 0.5$ in pp collisions, in most central (0-5%), and peripheral (40-60%) Pb-Pb collisions by PACIAE model. The key model parameters are determined by fitting pion and proton p_T spectra data. The p_T spectra of deuteron (d, \bar{d}) are also simulated in this work using the PACIAE + DCPC model. Then, the nuclear modification factors (R_{AA}) of charged pions, (anti)protons, and (anti)deuteron, as well as, their yield ratios, double R_{AA}^D ratios with $|y| < 0.5$ in peripheral (40-60%) and central (0-5%) Pb-Pb collisions at $\sqrt{s_{NN}} = 2.76$ TeV have been studied using the PACIAE + DCPC model. It is found that the R_{AA} distribution of light (anti)nuclei (d, \bar{d}) is similar to that of hadrons (π^\pm, p, \bar{p}), and the R_{AA} of anti-particles is the same as that of particles. The suppression of R_{AA} at high- p_T strongly depends on event centrality and mass of the particles.

It is interesting that there are no differences in nuclear modification between particles and antiparticles in this work. In the PACIAE and DCPC models, there is no equilibrium assumption between particles and antiparticles. It simulates dynamically the whole relativistic heavy-ion collision process from the initial partonic stage to the hadronic final state via the parton evolution, hadronization, and hadron evolution according to copious dynamical ingredients (assumptions) introduced reasonably. Therefore it is parallel to the experimental nucleus-nucleus collision. These dynamics correctly describe the particle, energy, and entropy. Messages brought by the produced particles in these transport (cascade) models are all dynamically generated. We do not apply any equilibrium condition in our study and therefore sees no particle and antiparticle difference in the simulation. Of course, further studies are required to model the system evolutions in more sophisticated ways.

Most of the results predicted by our theory model are consistent with existing experimental results, while oth-

ers are somewhat different, such as the R_{AA} distribution of charged pions at the high- p_T . Therefore, it is necessary to improve the model.

V. ACKNOWLEDGMENT

This work was supported by the NSFC(11475149, 11775094, 11905188), as well as support from the high-

performance computing platform of China University of Geosciences. The authors thank Prof. Che-Ming Ko for very helpful discussions.

-
- [1] ALICE Collaboration, B. Abelev, et al., Phys. Lett. B **736**, 196 (2014). doi: <https://doi.org/10.1016/j.physletb.2014.07.011>.
- [2] ALICE Collaboration, J. Adam, et al., Phys. Rev. C **93**, 034913 (2016). doi: [10.1103/PhysRevC.93.034913](https://doi.org/10.1103/PhysRevC.93.034913).
- [3] ALICE Collaboration, S. Acharya, et al., Phys. Rev. C **97**, 024615 (2018). doi: [10.1103/PhysRevC.97.024615](https://doi.org/10.1103/PhysRevC.97.024615).
- [4] ALICE Collaboration, B. Abelev, et al., Phys. Rev. C **88**, 044910 (2013). doi: [10.1103/PhysRevC.88.044910](https://doi.org/10.1103/PhysRevC.88.044910).
- [5] ALICE Collaboration, B. Abelev, et al., Phys. Rev. Lett. **111**, 222301 (2013). doi: [10.1103/PhysRevLett.111.222301](https://doi.org/10.1103/PhysRevLett.111.222301).
- [6] ALICE Collaboration, J. Adam, et al., Phys. Rev. C **93**, 024917 (2016). doi: [10.1103/PhysRevC.93.024917](https://doi.org/10.1103/PhysRevC.93.024917).
- [7] ALICE Collaboration, S. Acharya, et al., Eur. Phys. J. C **77**(10), 658 (2017). doi: [10.1140/epjc/s10052-017-5222-x](https://doi.org/10.1140/epjc/s10052-017-5222-x).
- [8] ALICE Collaboration, J. Adam, et al., Phys. Lett. B **754**, 360 (2016). doi: <https://doi.org/10.1016/j.physletb.2016.01.040>.
- [9] PHENIX Collaboration, K. Adcox, et al., Phys. Rev. Lett. **88**, 022301 (2001). doi: [10.1103/PhysRevLett.88.022301](https://doi.org/10.1103/PhysRevLett.88.022301).
- [10] STAR Collaboration, C. Adler, et al., Phys. Rev. Lett. **89**, 202301 (2002). doi: [10.1103/PhysRevLett.89.202301](https://doi.org/10.1103/PhysRevLett.89.202301).
- [11] STAR Collaboration, J. Adams, et al., Phys. Rev. Lett. **91**, 172302 (2003). doi: [10.1103/PhysRevLett.91.172302](https://doi.org/10.1103/PhysRevLett.91.172302).
- [12] M. Gyulassy, M. Plümer, Phys. Lett. B **243**(4), 432 (1990). doi: [https://doi.org/10.1016/0370-2693\(90\)91409-5](https://doi.org/10.1016/0370-2693(90)91409-5).
- [13] M. Gyulassy, X.N. Wang, Nucl. Phys. B **420**, 583 (1994). doi: [10.1016/0550-3213\(94\)90079-5](https://doi.org/10.1016/0550-3213(94)90079-5).
- [14] E.K. Wang, X.N. Wang, Phys. Rev. Lett. **89**, 162301 (2002). doi: [10.1103/PhysRevLett.89.162301](https://doi.org/10.1103/PhysRevLett.89.162301).
- [15] PHENIX Collaboration, K. Adcox, et al., Nucl. Phys. A **757**(1), 184 (2005). doi: <https://doi.org/10.1016/j.nuclphysa.2005.03.086>.
- [16] STAR Collaboration, J. Adams, et al., Nucl. Phys. A **757**(1), 102 (2005). doi: <https://doi.org/10.1016/j.nuclphysa.2005.03.085>.
- [17] ALICE Collaboration, K. Aamodt, et al., Phys. Lett. B **696**(1), 30 (2011). doi: <https://doi.org/10.1016/j.physletb.2010.12.020>.
- [18] ALICE Collaboration, B. Abelev, et al., Phys. Lett. B **720**(1), 52 (2013). doi: <https://doi.org/10.1016/j.physletb.2013.01.051>.
- [19] CMS Collaboration, S. Chatrchyan, et al., Eur. Phys. J. C **72**(3), 1945 (2012). doi: [10.1140/epjc/s10052-012-1945-x](https://doi.org/10.1140/epjc/s10052-012-1945-x).
- [20] B. Alver, B.B. Back, M.D. Baker, et al., Phys. Rev. C **77**, 014906 (2008). doi: [10.1103/PhysRevC.77.014906](https://doi.org/10.1103/PhysRevC.77.014906).
- [21] J. Casalderrey-Solana, C.A. Salgado, Acta Phys. Pol. B **38**(12), 3731 (2007). doi: [10.1016/j.tsf.2007.07.139](https://doi.org/10.1016/j.tsf.2007.07.139).
- [22] ALICE collaboration, S. Acharya, et al., J. High Energy Phys. **2018**(11), 13 (2018). doi: [10.1007/JHEP11\(2018\)013](https://doi.org/10.1007/JHEP11(2018)013).
- [23] J.H. Chen, D. Keane, Y.G. Ma, et al., Phys. Rep. **760**, 1 (2018). doi: [10.1016/j.physrep.2018.07.002](https://doi.org/10.1016/j.physrep.2018.07.002).
- [24] P. Braun-Munzinger and B. Dönigus, Nucl. Phys. A **987**, 144(2019). doi: [10.1016/j.nuclphysa.2019.02.006](https://doi.org/10.1016/j.nuclphysa.2019.02.006).
- [25] S. Bass, M. Belkacem, M. Bleicher, et al., Prog. Part. Nucl. Phys. **41**, 255 (1998). doi: [10.1016/S0146-6410\(98\)00058-1](https://doi.org/10.1016/S0146-6410(98)00058-1).
- [26] Z.W. Lin, C.M. Ko, B.A. Li, et al., Phys. Rev. C **72**, 064901 (2005). doi: [10.1103/PhysRevC.72.064901](https://doi.org/10.1103/PhysRevC.72.064901).
- [27] J. Weil, V. Steinberg, J. Staudenmaier, et al., Phys. Rev. C **94**, 054905 (2016). doi: [10.1103/PhysRevC.94.054905](https://doi.org/10.1103/PhysRevC.94.054905).
- [28] C.S. Zhou, Y.G. Ma, S. Zhang, Eur. Phys. J. A **52**(12), 354 (2016). doi: [10.1140/epja/i2016-16354-0](https://doi.org/10.1140/epja/i2016-16354-0).
- [29] N. Shah, Y.G. Ma, J.H. Chen, et al., Phys. Lett. B **754**, 6 (2016). doi: <https://doi.org/10.1016/j.physletb.2016.01.005>.
- [30] P. Liu, J.H. Chen, Y.G. Ma, et al., Nucl. Sci. Technol. **28**, 55 (2017). doi: [10.1007/s41365-017-0207-x](https://doi.org/10.1007/s41365-017-0207-x).
- [31] L.L. Zhu, C.M. Ko, X.J. Yin, Phys. Rev. C **92**, 064911 (2015). doi: [10.1103/PhysRevC.92.064911](https://doi.org/10.1103/PhysRevC.92.064911).
- [32] W.B. Zhao, L.L. Zhu, H. Zheng, et al., Phys. Rev. C **98**, 054905(2018). doi: [10.1103/PhysRevC.98.054905](https://doi.org/10.1103/PhysRevC.98.054905).
- [33] K.J. Sun, C.M. Ko, B. Dönigus, Phys. Lett. B **792**, 132 (2019). doi: [10.1016/j.physletb.2019.03.033](https://doi.org/10.1016/j.physletb.2019.03.033).
- [34] R.Q. Wang, J. Song, G. Li, et al., Chinese Phys. C **43**, 024101 (2019). doi: [10.1088/1674-1137/43/2/024101](https://doi.org/10.1088/1674-1137/43/2/024101).
- [35] H. Liu, D.W. Zhang, S. He, et al., Phys. Lett. B **805**, 135452 (2020). doi: [10.1016/j.physletb.2020.135452](https://doi.org/10.1016/j.physletb.2020.135452).
- [36] V. Vovchenko, B. Dönigus, and H. Stöcker, Phys. Lett. B **785**, 171 (2018). doi: [10.1016/j.physletb.2018.08.041](https://doi.org/10.1016/j.physletb.2018.08.041).
- [37] A. Andronic, P. Braun-Munzinger, K. Redlich, et al., Nature **561**, 321 (2018). doi: [10.1038/s41586-018-0491-6](https://doi.org/10.1038/s41586-018-0491-6).
- [38] D. Oliinychenko, L.G. Pang, H. Elfner, et al., Phys. Rev. C **99**, 044907 (2019). doi: [10.1103/PhysRevC.99.044907](https://doi.org/10.1103/PhysRevC.99.044907).
- [39] F. Bellini and A.P. Kalweit, Phys. Rev. C **99**, 054905 (2019). doi: [10.1103/PhysRevC.99.054905](https://doi.org/10.1103/PhysRevC.99.054905).
- [40] B.H. Sa, D.M. Zhou, Y.L. Yan, et al., Comput. Phys. Commun. **183**(2), 333 (2012). doi: [10.1016/j.cpc.2011.08.021](https://doi.org/10.1016/j.cpc.2011.08.021).
- [41] Y.L. Yan, G. Chen, X.M. Li, et al., Phys. Rev. C **85**, 024907 (2012). doi: [10.1103/PhysRevC.85.024907](https://doi.org/10.1103/PhysRevC.85.024907).

- [42] J.L. Wang, D.K. Li, H.J. Li, et al., *Int. J. Mod. Phys. E* **23**(12), 1450088 (2014). doi: [10.1142/S0218301314500888](https://doi.org/10.1142/S0218301314500888).
- [43] G. Chen, Y.L. Yan, D.S. Li, et al., *Phys. Rev. C* **86**, 054910 (2012). doi: [10.1103/PhysRevC.86.054910](https://doi.org/10.1103/PhysRevC.86.054910).
- [44] G. Chen, H. Chen, J. Wu, et al., *Phys. Rev. C* **88**, 034908 (2013). doi: [10.1103/PhysRevC.88.034908](https://doi.org/10.1103/PhysRevC.88.034908).
- [45] G. Chen, H. Chen, J.L. Wang, et al., *J. Phys. G: Nucl. Part. Phys.* **41**(11), 115102 (2014). doi: [10.1088/0954-3899/41/11/115102](https://doi.org/10.1088/0954-3899/41/11/115102).
- [46] Z.L. She, G. Chen, H.G. Xu, et al., *Eur. Phys. J. A* **52**(4), 93 (2016). doi: [10.1140/epja/i2016-16093-2](https://doi.org/10.1140/epja/i2016-16093-2).
- [47] Z.J. Dong, Q.Y. Wang, G. Chen, et al., *Eur. Phys. J. A* **54**(9), 144 (2018). doi: [10.1140/epja/i2018-12580-8](https://doi.org/10.1140/epja/i2018-12580-8).
- [48] F.X. Liu, G. Chen, Z.L. She, et al., *Phys. Rev. C* **99**, 034904 (2019). doi: [10.1103/PhysRevC.99.034904](https://doi.org/10.1103/PhysRevC.99.034904).
- [49] F.X. Liu, G. Chen, Z.L. She, et al., *Eur. Phys. J. A* **55**(9), 160 (2019). doi: [10.1140/epja/i2019-12851-x](https://doi.org/10.1140/epja/i2019-12851-x).
- [50] T. Sjöstrand, S. Mrenna, P. Skands, *J. High Energy Phys.* **2006**(05), 026 (2006). doi: [10.1088/1126-6708/2006/05/026](https://doi.org/10.1088/1126-6708/2006/05/026).
- [51] B. Combridge, J. Kripfganz, J. Ranft, *Phys. Lett. B* **70**(2), 234 (1977). doi: [https://doi.org/10.1016/0370-2693\(77\)90528-7](https://doi.org/10.1016/0370-2693(77)90528-7).